JOURNAL OF AIRCRAFT
Vol. 40, No. 1, January–February 2003

Characteristics of Compressible Rectangular Cavity Flows

K. Chung*
National Cheng Kung University, Tainan 711, Taiwan, Republic of China

Experiments are performed to study the effect of cavity geometry and Mach number on the characteristics of compressible rectangular cavity flows. The study indicates that the corresponding length-to-depth ratio for the open- and transitional-type cavities increases with higher freestream Mach number. The depth-to-incoming boundary-layer thickness ratio is another important parameter to define the type of the cavity flow. The upstream influence region is minimized with the presence of a cavity, and larger downstream influence region is observed for the transitional-closed- and closed-type cavities. The distributions of surface pressure fluctuations show similar trend as those of static pressure distributions. The amplitude of surface pressure fluctuations increases toward the rear face for an open-type cavity, whereas a minor peak near the middle of the cavity floor is observed for a closed-type cavity. A transitional-type cavity induces more intense surface pressure fluctuations at the cavity floor. Higher levels of pressure fluctuations near the rear face are observed at higher Mach numbers for the transitional- and open-type cavities.

Nomenclature

C_p	=	static pressure coefficient, $(p_w - p_\infty)/q_\infty$
$C_{\sigma p}$	=	fluctuating pressure coefficient, $(\sigma_p - \sigma_{p,\infty})/q_\infty$
D	=	cavity depth
L	=	cavity length
M	=	Mach number
p_w	=	surface static pressure
q_∞	=	freestream dynamic pressure
W	=	cavity width
x	=	streamwise distance
δ_0	=	incoming boundary-layer thickness
σ_p	=	standard deviation of raw pressure signal

I. Introduction

THE presence of a cavity in a surface bounding flow may produce intense, periodic, but not necessarily simple harmonic pressure fluctuations.[1] Previous studies indicated that the presence of a cavity in a surface bounding flow changes the mean surface pressure distribution and induces high-intensity pressure fluctuations in and near the cavity.[2–6] This may result in structural deflection, strong acoustic radiation, increased drag, or poor optical characteristics for an aerodynamic window. At supersonic speeds, it is well known that the boundaries of cavity flows are mainly dependent on the length-to-depth ratio L/D (Ref. 5). An open-type cavity ($L/D \leq 10$) is characterized by an uniform static pressure distribution with high-intensity acoustic tones. As the L/D increases ($10 < L/D < 13$), the flowfield changes from open- to transitional-type cavity flow and can be identified by a change in the static pressure distribution in the aft portion of the cavity. At $L/D \geq 13$ (closed-type cavity), the static pressure distribution shows an inflection point near the center of the cavity floor followed by a plateau region, which is due to the shear layer attachment. A study by Disimile and Orkwis[7] further indicated that the characteristics of the flow appear to depend on the shape of the cavity, incoming Mach number, Reynolds number, and the characteristics of the incoming boundary layer.

At subsonic and transonic speeds, a cavity flow can also be classified as open, transitional, or closed type.[6] The primary controlling parameter for a cavity flow is the length-to-depth ratio. The boundary between open- and transitional-type cavities occurs at $L/D \approx 6$–8. As L/D increases, the surface pressure distribution changes from concave up to concave down in the aft portion of the cavity, which is considered as the transitional-open-type flow. The transitional-closed-type flow can be visualized when the surface pressure distribution gradually changes to one marked by a uniform increase from negative values near the front face to large positive values near the aft face with increasing L/D (Ref. 8). The switch from the transitional- to the closed-type cavity flow is observed from $L/D \geq 9$ up to $L/D \geq 15$, which is dependent on the Mach number and cavity configuration.[6] Furthermore, a cavity flow is characterized as a strong self-sustained oscillation, which is associated with the vortices shedding from the leading edge, characteristics of the shear layer, and movement of the trailing-edge vortex. When the cavity is long enough, the oscillation is governed by the longitudinal mode. The disturbances are transferred downstream of the cavity, and the magnitude decreases gradually with increasing L/D due to the change in the characteristics of the shear layer.[3]

Presence of a cavity would have a strong effect on the unsteadiness and aerodynamic characteristics of the upstream or downstream aerodynamic components, for example, the cutouts, gaps, or grooves upstream of the deflected control surface. Investigation on the extent of upstream and downstream influence of a cavity is essentially required. Furthermore, full coupling of the structural vibration to the surrounding fluid has been shown to be critical in previous studies. The pressure fluctuations inside the cavity consist mainly of discrete resonances whose frequency, amplitude, and harmonic properties depend on the cavity geometry and external flow conditions.[9] Previous study indicated that the oscillation frequencies could be predicted by the modified Rossiter equation reasonably well (see Ref. 10). However, measurements of the amplitude of the fluctuating pressure in and near the cavities are relatively lacking. There is no simple analytic formula to predict the amplitude of pressure fluctuations. Further investigation is required.

The present study investigates the effects of the Mach number ($M_\infty = 0.33$, 0.62, and 0.82), the length-to-depth ratio ($L/D = 2.43$–43.00) and the depth-to-incoming boundary-layer thickness ratio ($D/\delta_0 = 0.122$–1.366) on the characteristics of compressible rectangular cavity flows. Measurements are conducted upstream, in the floor, and downstream of the cavities. The type of cavity flow and the upstream and downstream influence regions are estimated based on the measurements of longitudinal mean pressure distributions. The unsteadiness of the flow in and near a cavity is also studied through the surface fluctuating pressure measurements to provide a better understanding of compressible cavity flows.

Received 1 March 2002; revision received 17 September 2002; accepted for publication 27 September 2002.

*Associate Research Fellow, Aerospace Science and Technology Research Center, Kueijen. Senior Member AIAA.

II. Experimental Technique

An experimental study of compressible rectangular cavity flows was conducted at the Aerospace Science and Technology Research Center/National Cheng Kung University (ASTRC/NCKU) transonic wind tunnel. The boundary layer is naturally developed along a flat plate ahead of a rectangular cavity. The mean and fluctuating pressures are obtained in the plate surface ahead of the cavity ($x/L < 0$), the cavity floor ($0 < x/L < 1$), and plate surface downstream of the cavity ($x/L > 1$). A brief description of the facility, data acquisition system, model, instrumentation and the test conditions is given next.

A. Transonic Wind Tunnel

The ASTRC/NCKU transonic wind tunnel is a blowdown type. The facility consists of the compressors, dryers, storage tanks, hydraulic system, and the tunnel. The dew point of the high-pressure air is maintained at $-40°$C under the normal operation condition, and the temperature drop is within 3°C during a 10-s run. A rotary perforated sleeve valve controls the setup of stagnation pressure, and the choke flaps are used to monitor the testing Mach number at subsonic conditions. The test section is 600 mm square and 1500 mm long, which is assembled with solid side walls and perforated top/bottom walls in the present study. Downstream of the test section, a model support strut is installed for sting mounted pitot probe survey.

B. Data Acquisition Systems and Instrumentation

Two data acquisition systems are available for the present experiments. The NEFF 620 system is used to record the test conditions and to monitor the experiments through the high-speed interface. For the surface pressure measurements, a host computer with CATALYST software controls the setup of LeCroy 6810 waveform recorders through a LeCroy 8901A interface. The dynamic pressure transducers (Kulite XCS-093-25A, B screen) are powered by a TES (Model 6102) dc power supply at 15.0 V, and the external amplifiers (Ecreon Model E713) are also used to improve the signal-to-noise ratio. With a gain of 20, the rolloff frequency is about 140 kHz. The output range of waveform recorders is adjusted with an optimum resolution, and the relative error of the mean pressure signals is estimated to be about 0.1%.

In addition, the outside diameter of the Kulite pressure transducers is 2.36 mm, and the pressure sensitive sensor is 0.97 mm in diameter. The natural frequency of pressure transducers is 200 kHz as quoted by the manufacturer. All of the pressure transducers are calibrated statically only and are flush mounted to minimize interference with the flow. Furthermore, the resolution of surface pressure fluctuation is limited by the finite size of pressure transducer. According to Corcos's criterion[11] ($f_{\max} = U_c/2\pi r$, where r is the radius of pressure transducer and U_c is the convection velocity), the maximum measurable frequencies are about 30, 55, and 70 kHz for $M_\infty = 0.33, 0.62$, and 0.82, respectively, assuming $U_c = 0.8U_\infty$. However, Perng and Dolling[12] indicated that the perforated screen of the Kulite pressure transducer may reduce the frequency response.

In the present experiments, the typical sampling rate is 200,000 samples/s. Each test record samples 131,072 data points for the statistical analysis and is divided into 32 data sets. The standard deviation (pressure fluctuation) of all of the data sets is calculated. The data analysis shows that the variations are estimated to be approximately 0.62% for C_p and 0.15% for $C_{\sigma p}$, which are considered as the uncertainty of experimental data.

C. Test Models

The test model (Fig. 1), consists of a flat plate mounted in the test section and an instrumentation plate with a rectangular cavity. The flat plate is 150 mm wide by 450 mm long and is supported by a single sting mounted on the bottom wall of the test section. There are 12 (150 mm square) instrumentation plates fabricated. The flat plate and an instrumentation plate are butted tightly together with cavity's front face located at 500 mm from the leading edge of flat plate. For the geometry of the cavities, the length-to-width ratio L/W is equal to 1 for all of the test cases, and the length-to-depth ratio L/D ranges from 2.43 to 43.00 (Table 1). The depth-to-boundary-layer thickness ratio ($0.122 \le D/\delta_0 \le 1.366$) increases with the depth of the cavity. One row of 19 pressure taps along the centerline of each instrumentation plate is drilled perpendicularly to the test surface. All of the pressure taps are 6.0 mm apart in the longitudinal direction and 2.5 mm in diameter. Because of the limited depth of the cavities, no pressure tap is available in the front or rear face.

Table 1 Geometry of the cavity

Cavity	L, mm	D, mm	W, mm
1	17	7	17
2	31	7	31
3	43	9.7	43
4	43	8	43
5	43	7	43
6	43	5	43
7	59	7	59
8	43	4	43
9	43	3.5	43
10	43	3	43
11	43	2	43
12	43	1	43

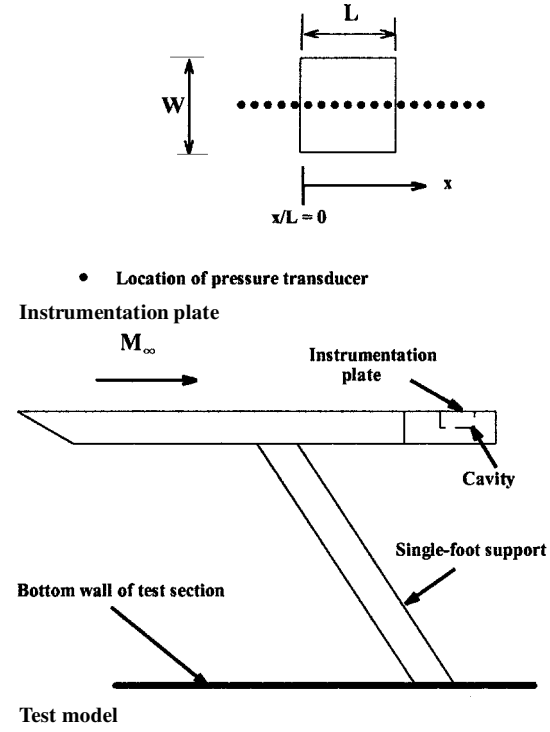

Fig. 1 Test configuration.

D. Test Conditions

The stagnation pressure and temperature are 172 ± 1 kPa (25.0 ± 0.15 psia) and room temperature, respectively, for all of the test cases. Undisturbed boundary layer surveys at 485 mm downstream of the flat plate leading edge (or 15 mm ahead of cavity front face) show that the normalized velocity profiles are full ($n \approx 7$–11 for velocity power law). In addition, the study by Miau et al.[13] showed that the transition of the boundary layer under the present test condition is close to the leading edge of the flat plate. These indicate the flow is turbulent at the measurement locations. The incoming boundary-layer thicknesses are 8.2, 7.3, and 7.1 ± 0.2 mm, and the Reynolds numbers based on the incoming boundary-layer thickness, Re_{δ_0}, are 9.84, 14.89, and 17.04×10^4 for $M_\infty = 0.33$, 0.62, and 0.82 ± 0.01.

III. Results and Discussion

A. Static Pressure Distributions

The static surface pressure distribution C_p at $M_\infty = 0.82$ is shown in Fig. 2. The sonic condition is also shown for reference. It appears

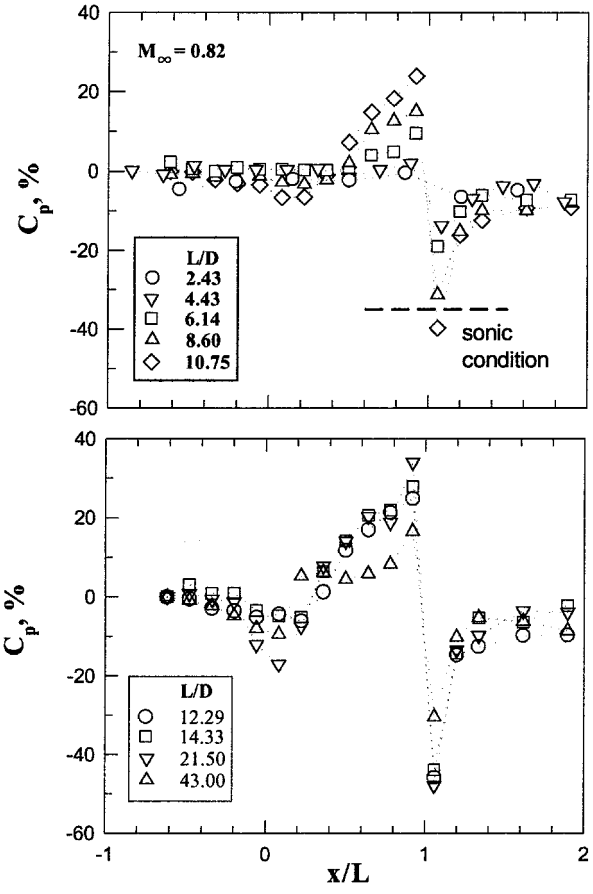

Fig. 2 Static pressure distributions, L/D effect.

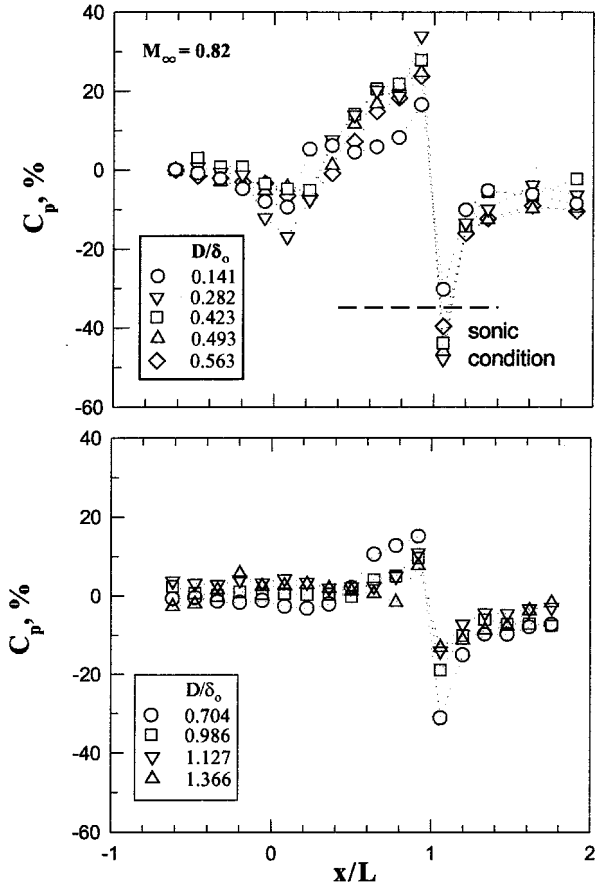

Fig. 3 Static pressure fluctuations, D/δ_0 effect.

that the C_p distributions at $L/D \leq 4.43$ resembles the typical pressure distribution of an open-type cavity flow, which shows slight upstream influence. The downstream influence region, which can be defined as the end of recovery process downstream of the rear face, is up to $x/L \leq 1.2$. At $L/D = 8.60$, the flow switches from the open-type cavity to the transitional-open-type cavity and is identified by the change of C_p in the aft portion of the cavity. As L/D ($= 10.75$ and 12.29) further increases, the leading-edge expansion is more significant, and the C_p increases from negative values to larger positive near the rear face. This corresponds to the transitional-closed-type cavity. A slower recovery process (downstream influence) is observed up to $x/L = 1.5$–1.6. At $L/D \geq 14.33$, the inflection of C_p distributions can be seen and moves upstream with increasing L/D. The downstream influence region ranges from $x/L = 1.3$ to 1.4.

At $M_\infty = 0.33$ and 0.62, the characteristics of C_p distributions are roughly the same as those at $M_\infty = 0.82$. However, early transition from open- to transitional-type cavities is observed at $L/D = 6.14$. Furthermore, the depth-to-incoming boundary-layer thickness ratio is another important parameter to define the type of the cavity flow. At supersonic speed, the boundary between transitional- and open-type cavities is at $D/\delta_0 \approx 0.57$ (Ref. 14). The present data at $M_\infty = 0.82$ are replotted with various D/δ_0 in Fig. 3. The flows appear to be the closed-type cavity for $D/\delta_0 \leq 0.423$, and the flow switches to the transitional-type cavity at $0.423 < D/\delta_0 < 0.986$. The boundary between transitional- and open-type cavities under the present test conditions ($D/\delta_0 \approx 0.704$–0.986) is considerably higher than that at supersonic speed. For the downstream influence, it is observed that the expansion downstream of the rear face is maximized at $D/\delta_0 \approx 0.423$ (the boundary between closed and transitional-closed cavities).

Furthermore, the distributions of static pressure upstream and downstream of a cavity could be used to characterize the interaction region of the compressible cavity flows, as shown in Fig. 4. It appears that variation of the upstream static pressure (or upstream influence) is minimized for all of the present test cases. Downstream of the rear face, the static pressure decreases with increasing L/D, and a stronger expansion is observed for the transitional- and closed-type cavities. The Mach number effect is significant only for the closed-type cavities, which implies larger downstream influence region at higher Mach numbers.

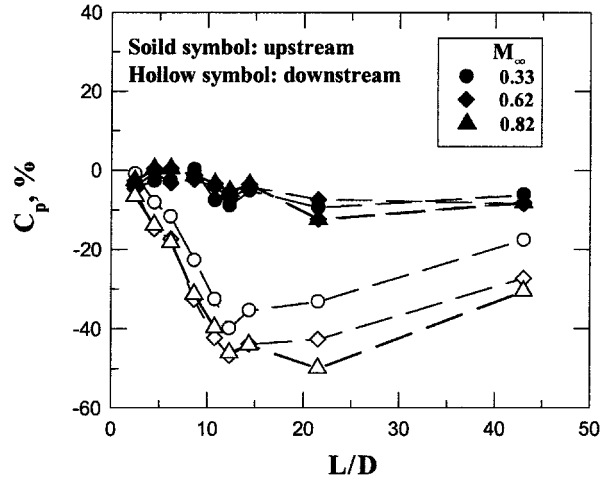

Fig. 4 Upstream and downstream static pressure.

B. Surface Pressure Fluctuations, L/D Effect

Distributions of surface pressure fluctuation $C_{\sigma p}$ at $M_\infty = 0.33$ are shown in Fig. 5. $C_{\sigma p}$ represents the relative normalized local surface pressure fluctuation with respect to the undisturbed flow. It appears that the levels of fluctuating pressure change only slightly at the plate surface upstream of the cavity (or $C_{\sigma p} \approx 0$) for all of the test cases. The upstream propagation of the disturbance with the presence of a cavity is minimized. This shows some disagreement

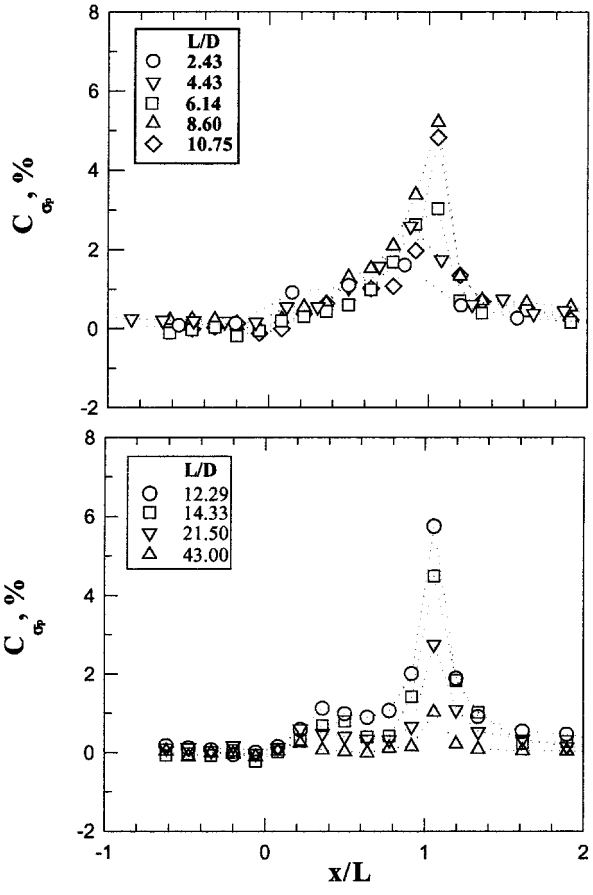

Fig. 5 Pressure fluctuations, $M_\infty = 0.33$.

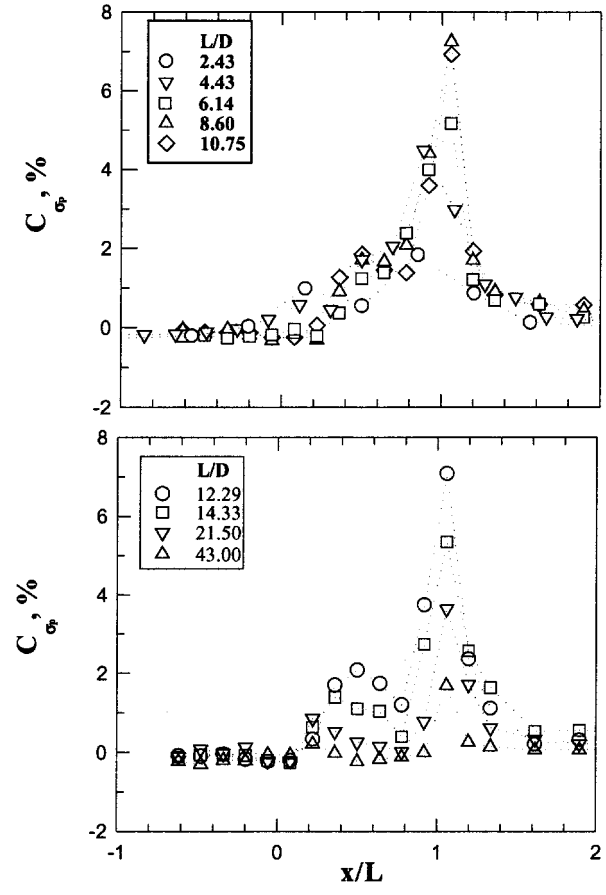

Fig. 6 Pressure fluctuations, $M_\infty = 0.62$.

with the observation at supersonic speed, in which the expansion over the leading edge of a cavity has stronger effect on the amplitude of pressure fluctuations at the plate surface upstream of the cavity.[13] Within the cavities, the $C_{\sigma p}$ distributions are L/D dependent. The amplitude of pressure fluctuation increases gradually and reaches a peak value ahead of the rear face for the open-type cavity ($L/D \leq 4.43$). Downstream of the cavity, $C_{\sigma p}$ decreases and approaches new equilibrium levels at $x/L \approx 1.3$–1.4. This indicates a larger interaction region than that obtained from the mean surface pressure measurements ($x/L \approx 1.2$). The common definition of the interaction region based on the mean surface pressure measurements may need to be refined. For the types of transitional-open ($L/D = 6.14$) and transitional-closed ($L/D = 8.60$–12.29) cavities, the $C_{\sigma p}$ distributions show the similar trend as the open-type cavity. However, a minor peak $C_{\sigma p}$ near the middle of the floor is observed for $L/D \geq 10.75$, and the location of peak pressure fluctuation is moved downstream of the rear face. The minor peak pressure fluctuation is considered due to the deflection or the reattachment of shear layer, and the movement of peak pressure fluctuation could be related to the mass addition and removal process for different types of cavity. Also note that the amplitude of peak pressure fluctuations $C_{\sigma p,\max}$ increases about 2–3% when the flow switches from the transitional-opentype to transitional-closedtype. Larger $C_{\sigma p,\max}$ may imply that the unsteady mass flow near the trailing edge is more significant for the transitional-closed-type cavity, which also induces a slower recovery process downstream of the rear face ($x/L \approx 1.5$–1.6). For $L/D \geq 14.33$ (closed-type cavity), the levels of $C_{\sigma p}$ at the cavity floor are in the form of uniform distributions. $C_{\sigma p,\max}$ decreases with L/D, and the disturbance with the presence of a cavity is limited near the rear face. The downstream interaction region at $L/D = 43.00$ is only up to $x/L \approx 1.2$.

For $M_\infty = 0.62$ (Fig. 6), the $C_{\sigma p}$ distributions for open ($L/D \leq 4.43$) and transitional-open ($L/D = 6.14$) cavities show similar trend as those at $M_\infty = 0.33$. However, the downstream influence regions are up to $x/L = 1.5$–1.6. For transitional-closedcavities ($L/D = 8.60$–12.29), the amplitude of $C_{\sigma p}$ downstream of the front face increases. A minor peak $C_{\sigma p}$ is observed near the middle of the floor and tends to move toward the front face with increasing L/D. This agrees with the observation of mean surface pressure measurements, in which the inflection of C_p distributions moves upstream with L/D. For the closed-type cavities, it appears that downstream propagation of the disturbance is less significant. For $M_\infty = 0.82$, the characteristics of pressure fluctuation distributions are roughly the same as the cases of $M_\infty = 0.62$. For the transitional-type cavities, slight damping of pressure fluctuations near the front face is observed which might correspond to the expansion of the flow into the cavity at the front edge.

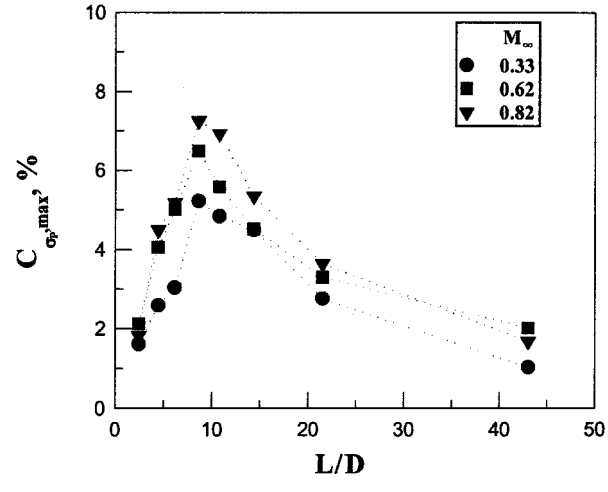

Fig. 7 Peak pressure fluctuations, *L/D* effect.

The peak pressure fluctuations $C_{\sigma p,\max}$ near the rear face are summarized in Fig. 7. It can be seen that $C_{\sigma p,\max}$ increases with

L/D and reaches the maximum at $L/D = 8.60$, which is up to 168 dB [sound pressure level $= 20 \log(\sigma_p/p_r)$, $p_r = 2 \times 10^{-5}$ N/m^2] at $M_\infty = 0.82$. Heller and Bliss[15] indicated that the onset of pressure fluctuations depends on the balance between the energy supplied by the external flow and the energy dissipated by viscous losses and acoustic radiation. The rear attachment point of the shear layer is continuously pulled into and out of the cavity. A net unsteady mass flow is produced, which consequently increase the amplitude of pressure fluctuations near the trailing edge. For the present test cases, the maximums of peak pressure fluctuation at $L/D = 8.60$ is considered due to the switch of open- and transitional-type cavities, which is essentially related to the mass addition/removal process near the trailing edge. Note that $C_{\sigma p,\max}$ is higher at $M_\infty = 0.62$ and 0.82 than that at $M_\infty = 0.33$. This implies that the mass addition/removal process is more pronounced with increasing Mach number. At larger L/D, $C_{\sigma p,\max}$ decreases and approaches the value of $C_{\sigma p,\infty}$ for the shallower cavities.

C. Surface Pressure Fluctuations, D/δ_0 Effect

Ahuja and Mendoza[9] investigated the effect of boundary-layer thickness for a two-dimensional cavity with fixed geometry ($L/D = 3.75$ and $M_\infty = 0.4$). It is found that all of the depth-mode cavity tones are reduced to the broadband level by decreasing L/δ (or D/δ) to about half its initial value ($L/\delta \approx 15$–26 and $D/\delta \approx 4$–7). To further understand the effect of incoming boundary-layer thickness on the characteristics of surface pressure fluctuation, the data are replotted with different D/δ_0. For the present experiment, L/δ_0 is fixed and D/δ_0 decreases for a shallower cavity. For $M_\infty = 0.33$ (Fig. 8), the upstream propagation of the disturbance is minimized except $D/\delta_0 > 1$, in which the upstream influence region is up to $x/L \approx -0.3$. Within the cavity, the characteristics of surface pressure fluctuation resemble the distribution of a transitional-closed- or closed-type cavity for $D/\delta_0 \leq 0.488$. $C_{\sigma p}$ increases initially and reaches a minor peak. A concave curvature is observed in the aft half of the cavity, followed by a rapid rise near the rear face, which

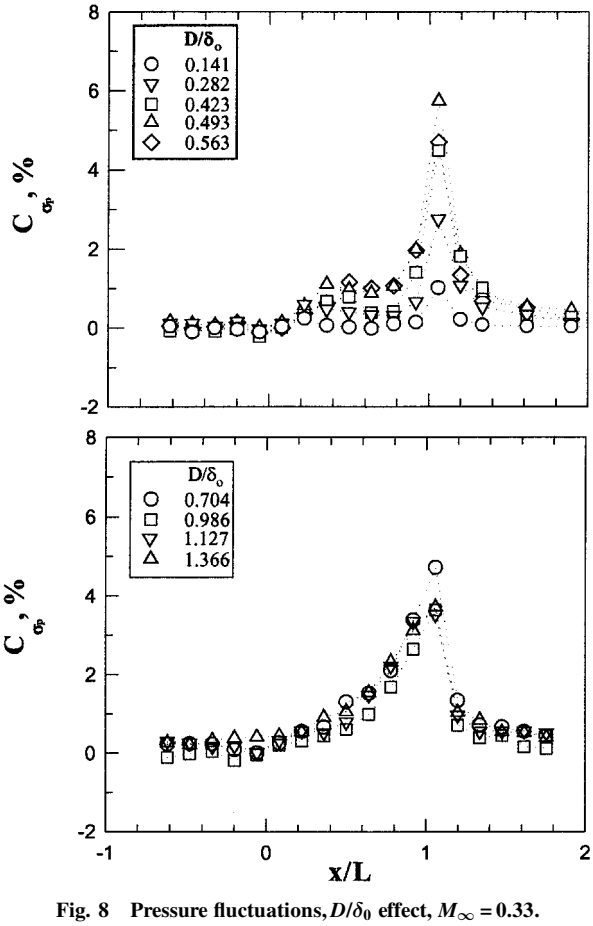

Fig. 8 Pressure fluctuations, D/δ_0 effect, $M_\infty = 0.33$.

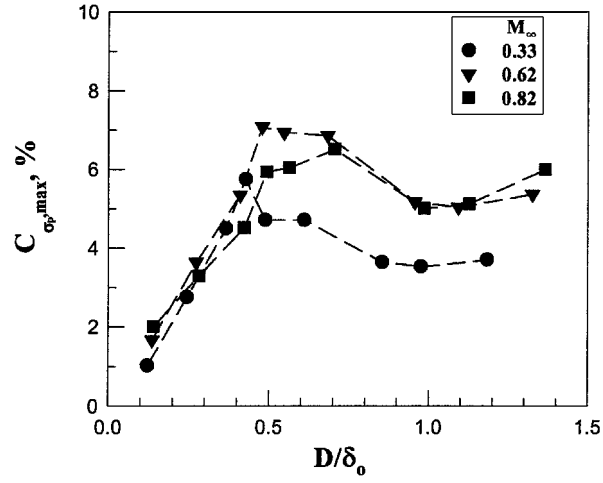

Fig. 9 Peak pressure fluctuations, D/δ_0 effect.

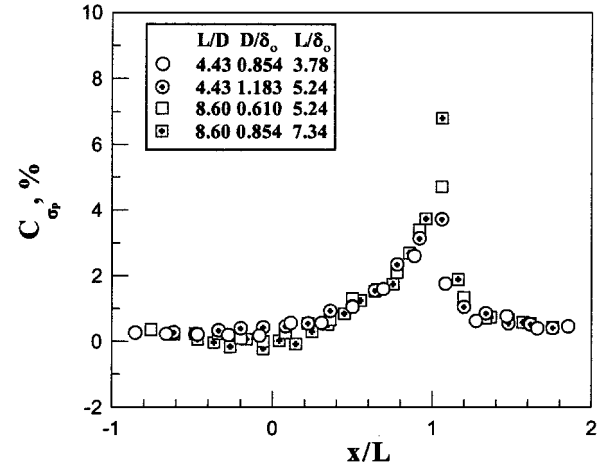

Fig. 10 Pressure fluctuations, D/δ_0 effect at given L/D and L/W, $M_\infty = 0.33$.

is related to the shear layer downward deflection.[3] The amplitude of $C_{\sigma p}$ in the cavity floor decreases slightly with a smaller D/δ_0, and the peak $C_{\sigma p}$ at the immediate downstream location for $D/\delta_0 = 0.122$ is about 5% less than that for $D/\delta_0 = 0.427$. A larger downstream interaction region is associated with a higher peak $C_{\sigma p}$. For $D/\delta_0 \geq 0.610$, this corresponds to the transitional-open- or open-type cavities. The effect of D/δ_0 on the levels of $C_{\sigma p}$ is minimized, and $C_{\sigma p}$ rises toward the rear face. The downstream interaction region is only up to $x/L = 1.3$–1.4. At $M_\infty = 0.62$ and 0.82, the distributions of surface pressure fluctuation show similar characteristics to those at $M_\infty = 0.33$. However, the minor peak is observed up to $D/\delta_0 = 0.704$. This indicates the Mach number effect on the boundary of the different type cavities.

The peak surface pressure fluctuations $C_{\sigma p,\max}$ for all of the test cases are summarized in Fig. 9. For $D/\delta_0 < 0.4$, the values of $C_{\sigma p,\max}$ are roughly the same for all three tested Mach numbers. The corresponding D/δ_0 with the maximums of peak pressure fluctuations ranging from 0.427 to 0.704 tends to increase with the Mach number. As mentioned in Sec. III.B, the maximum of peak pressure fluctuations corresponds to the switch of different type cavities. This indicates that the critical D/δ_0 (or boundary between open- and transitional-type cavities) are Mach number dependent under the present test conditions. For $D/\delta_0 \geq 0.5$ (transitional- and open-type cavities), it can be seen that the amplitude of $C_{\sigma p,\max}$ at $M_\infty = 0.62$ and 0.82 is considerably higher than that at $M_\infty = 0.33$.

To further identify the effect of D/δ_0 and L/δ_0 on the compressible cavity flow, experiments at constant L/D and L/W were conducted (Figs. 10 and 11). D/δ_0 and L/δ_0 change with the depth and the length of the cavity. For the open- ($L/D = 4.43$) or

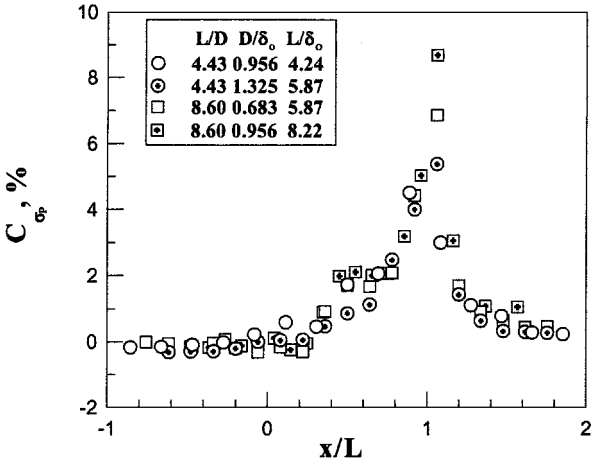

Fig. 11 Pressure fluctuations, D/δ_0 effect at given L/D and L/W, $M_\infty = 0.62$.

transitional-($L/D = 8.60$) type cavities, D/δ_0 and L/δ_0 show a minor effect on the distributions of surface pressure fluctuation for all of the test cases except the peak pressure fluctuations near the rear face. The peak pressure fluctuations tend to increases at larger D/δ_0 and L/δ_0. This is not consistent with the experimental data of Ahuja and Mendoza.[9] It is considered that the effectiveness of decreasing D/δ_0 or L/δ_0 on reducing the cavity pressure fluctuations could depend on the different mode of acoustic tones in a cavity flow.

IV. Conclusions

The present investigation examined the effects of Mach number, length-to-depth ratio, and depth-to-boundary-layer thickness ratio on the characteristics of compressible rectangular cavity flows. The results of this study are summarized as follows.

1) The boundary of open- and transitional-type cavities is Mach number dependent and occurs at $L/D \approx 6.14$–8.60 or $D/\delta_0 \approx 0.704$–0.958. The flow switches to the closed-type cavity at $L/D \approx 14.33$ or $D/\delta_0 \approx 0.366$–0.423.

2) Upstream propagation of the disturbance with the presence of a cavity is minimized at subsonic speeds, and larger downstream influence regions are observed for the transitional- and closed-type cavities, which are up to 60% of the cavity length.

3) The distributions of surface pressure fluctuation follow a trend similar to those of mean surface pressure distributions. The values of surface pressure fluctuation rise monotonically toward the rear face for an open-type cavity, whereas a minor peak near the middle of the cavity floor is observed for a closed-type cavity.

4) The levels of peak pressure fluctuation are maximized due to the switch of open- and transitional-type cavities, particularly at higher Mach number.

5) For a given length-to-depth ratio, the effect of D/δ_0 or L/δ_0 is significant only on the amplitude of peak pressure fluctuation near the rear face but not on the levels of surface pressure fluctuations within the cavity.

Acknowledgments

The author acknowledges the financial support of the National Science Council under contract NSC 88-2612-E-006-004. Thanks are also extended for the technical support of the Aerospace Science and Technology Research Center/National Cheng Kung University technical staffs in the operation of the experimental facility.

References

[1]Bilanin, A., and Covert, E., "Estimation of Possible Excitation Frequencies for Shallow Rectangular Cavities," *AIAA Journal*, Vol. 11, No. 3, 1973, pp. 347–351.

[2]Rockwell, D., "Prediction of Oscillation Frequencies for Unstable Flow Past Cavities," *Journal of Fluids Engineering*, Vol. 99, No. 3, 1977, pp. 294–300.

[3]Zhang, X., and Edwards, J. A., "An Investigation of Supersonic Cavity Flows Driven by Thick Shear Layers," *Aeronautical Journal*, Vol. 94, No. 940, 1990, pp. 355–364.

[4]Pereia, J. C. F., and Sousa, J. M. M., "Experimental and Numerical Investigation of Flow Oscillations in a Rectangular Cavity," *Journal of Fluids Engineering*, Vol. 117, No. 2, 1995, pp. 68–74.

[5]Stallings, R. L., Jr., and Wilcox, F. J., Jr., "Experimental Cavity Pressure Distributions at Supersonic Speeds," NASA TP-2683, June 1987.

[6]Plentovich, E. B., Stallings, R. L., Jr., and Tracy, M. B., "Experimental Cavity Pressure Measurements at Subsonic and Transonic Speeds," NASA TP-3358, 1993.

[7]Disimile, P., and Orkwis, P., "Effect of Yaw of Pressure Oscillation Frequency with Rectangular Cavity at Mach 2," *AIAA Journal*, Vol. 35, No. 7, 1997, pp. 1323–1325.

[8]Tracy, M. B., and Plentovich, E. B., "Cavity Unsteady-Pressure Measurements at Subsonic and Transonic Speeds," NASA TP-3669, Dec. 1997.

[9]Ahuja, K. K., and Mendoza, J., "Effects of Cavity Dimensions, Boundary Layer, and Temperature on Cavity Noise with Emphasis on Benchmark Data to Validate Computational Aeroacoustic Codes," NASA CR-4653, April 1995.

[10]Heller, H. H., Holmes, D. G., and Covert, E. E., "Flow-Induced Pressure Oscillations in Shallow Cavities," *Journal of Sound and Vibration*, Vol. 18, No. 4, 1971, pp. 545–663.

[11]Corcos, G., "Resolution of Pressure in Turbulence," *Journal of the Acoustical Society of America*, Vol. 35, No. 2, 1963, pp. 192–199.

[12]Perng, S., and Dolling, D., "Passive Control of Pressure Oscillations in Hypersonic Cavity flow," AIAA Paper 96-0444, Jan. 1996.

[13]Miau, J., Cheng, J., Chung, K., and Chou, J., "The Effect of Surface Roughness on the Boundary Layer Transition," *Proceedings of the 7th International Symposium in Flow Modeling and Turbulent Measurement*, Tianan, Taiwan, ROC, Oct. 1998, pp. 609–616.

[14]Chung, K., "Characteristics of Transonic Rectangular Cavity Flows," *Journal of Aircraft*, Vol. 37, No. 3, 2000, pp. 463–468.

[15]Heller, H., and Bliss, D., "The Physical Mechanism of Flow-Induced Pressure Fluctuations in Cavities and Concepts for Their Suppression," AIAA Paper 75-491, March 1975.